Dynamics of the spin-½ isotropic $XY$ chain in a transverse field



2000 J. Phys. A: Math. Gen. 33 3063

(http://iopscience.iop.org/0305-4470/33/16/301)

J. Phys. A: Math. Gen. **33** (2000) 3063–3080. Printed in the UK PII: S0305-4470(00)07896-3

# Dynamics of the spin-$\frac{1}{2}$ isotropic $XY$ chain in a transverse field

Oleg Derzhko†‡‖, Taras Krokhmalskii† and Joachim Stolze§

† Institute for Condensed Matter Physics, 1 Svientsitskii Street, L'viv-11, 79011, Ukraine
‡ Chair of Theoretical Physics, Ivan Franko National University in L'viv, 12 Drahomanov Street, L'viv-5, 79005, Ukraine
§ Institut für Physik, Universität Dortmund, 44221 Dortmund, Germany

E-mail: derzhko@icmp.lviv.ua, krokhm@icmp.lviv.ua and stolze@physik.uni-dortmund.de

Received 16 September 1999, in final form 4 February 2000

**Abstract.** Dynamic $xx$ and $xy$ spin pair correlation functions for the isotropic spin-$\frac{1}{2}$ $XY$ chain are calculated numerically for long open chains in the presence of a transverse ($z$) magnetic field at finite temperature. From these data the first numerical results for the dynamic structure factors $S_{xx}(\kappa, \omega)$ and $S_{xy}(\kappa, \omega)$ are obtained and compared with the known results for $S_{zz}(\kappa, \omega)$. While $S_{zz}(\kappa, \omega)$ is restricted to certain regions in the $(\kappa, \omega)$-plane $S_{xx}(\kappa, \omega)$ and $S_{xy}(\kappa, \omega)$ are not. Nevertheless, the numerical results show that the latter structure factors are quite small outside the regions defined by $S_{zz}(\kappa, \omega)$ and moreover, that they may in many circumstances, especially at low temperature, be approximately described by a small number of broadened excitation branches.

## 1. Introduction

Quantum spin chains have been a subject of intense theoretical interest for decades, because the competition between ordering and thermal or quantum fluctuations generates a wealth of interesting phenomena, both static and dynamic, which may be observed experimentally in a variety of compounds made available by progress in preparation techniques. One of the simplest quantum spin chains is the spin-$\frac{1}{2}$ $XY$ chain introduced in the pioneering paper by Lieb *et al* [1], who pointed out the relation between the spin model and noninteracting spinless fermions that makes many (but by no means all) properties of this model amenable to analytical calculations. Many materials can be reasonably described by different special cases of the spin-$\frac{1}{2}$ $XY$ chain, for example, $Cs(H_{1-x}D_x)_2PO_4$, $PbH_{1-x}D_xPO_4$, $PrCl_3$, $CsCuCl_3$, $CsCu_{1-x}Mn_xCl_3$, $J$-aggregates etc [2–10]. Dynamic spin correlations in these materials can be measured by neutron scattering and magnetic resonance techniques. The calculation of dynamic spin correlations can be nontrivial even in the simple case of the $XY$ chain. The time-dependent correlation function of the $z$ components of two spins corresponds to a density correlation function of noninteracting spinless fermions. This relation was exploited early on [11] to calculate that correlation function. In contrast, the dynamic correlation functions of $x$ or $y$ spin components map to complicated *many*-body correlation functions of the spinless fermions. Consequently, analytical results on these correlation functions are restricted to limiting or asymptotic cases, such as zero temperature ($\beta = \infty$) and large spatial separation

‖ Corresponding author.

0305-4470/00/163063+18$30.00  

between spins [12], infinite temperature ($\beta = 0$) [13–15], $\beta = \infty$, strong external field and spins close to the boundary of a semi-infinite isotropic $XY$ chain [16], and $\beta = \infty$ long-time asymptotics for the isotropic $XY$ chain without transverse field and the transverse Ising chain at the critical field [17, 18]. More recent analytical approaches [19–23] to these correlation functions have resulted in fairly simple expressions for the asymptotic correlations of the isotropic $XY$ chain at finite temperature [20] (see formulae (9), (10) below). In addition, numerical approaches [24–27] have been employed to study the dynamic $x$ and $y$ spin pair correlations.

It should be stressed, however, that no results at all are known for the complete wavevector and frequency dependences of the dynamic structure factors corresponding to these correlations in the isotropic $XY$ chain at arbitrary temperature. In this paper we present the first such results. This complements our recent study [27] of dynamic structure factors and susceptibilities of the transverse Ising chain, the maximally anisotropic case of the general $XY$ chain.

In section 2 we sketch the numerical method used to calculate time-dependent spin pair correlation functions in long open-ended chains. The results are compared to available exact or asymptotic results; in addition, the influence of finite-size effects is discussed. Section 3 contains the main results of our paper, namely the dynamic structure factors $S_{xx}(\kappa, \omega)$ and $S_{xy}(\kappa, \omega)$ for various values of the transverse field and the temperature. We compare the new results for $S_{xx}(\kappa, \omega)$ to the well known $S_{zz}(\kappa, \omega)$ and point out similarities and differences. In section 4 we discuss an experimental application reconsidering the theoretical prediction for the temperature dependence of the spin–spin relaxation time in $PrCl_3$ [7].

## 2. The method

Consider $N$ spins one-half governed by the following Hamiltonian:

$$H = \Omega \sum_{n=1}^{N} s_n^z + J \sum_{n=1}^{N-1} (s_n^x s_{n+1}^x + s_n^y s_{n+1}^y) \tag{1}$$

where $\Omega$ is the transverse field and $J$ is the exchange interaction between neighbouring sites. Using a Jordan–Wigner transformation [1] to map the spin raising and lowering operators $s_n^{\pm} = s_n^x \pm \mathrm{i}s_n^y$ to Fermi operators $c_n^+$, $c_n$ and then making a linear transformation $\eta_k^+ = \sum_{n=1}^{N} g_{kn} c_n^+$ one finds that Hamiltonian (1) becomes $H = \sum_{k=1}^{N} \Lambda_k (\eta_k^+ \eta_k - \frac{1}{2})$, $\{\eta_k, \eta_q^+\} = \delta_{kq}$, $\{\eta_k, \eta_q\} = \{\eta_k^+, \eta_q^+\} = 0$ if the unknown coefficients of the linear transformation $g_{kn}$ satisfy the set of equations

$$\sum_{j=1}^{N} g_{kj} A_{js} = \Lambda_k g_{ks} \qquad \sum_{j=1}^{N} g_{kj} g_{qj} = \delta_{kq} \qquad \sum_{k=1}^{N} g_{kj} g_{kn} = \delta_{jn} \tag{2}$$

where $A_{ij} = \Omega \delta_{ij} + \frac{1}{2} J (\delta_{j,i+1} + \delta_{j,i-1})$.

The spin operators can be represented in terms of auxiliary operators $\varphi_n^{\pm}$, namely, $s_n^x = \frac{1}{2} \varphi_1^+ \varphi_1^- \ldots \varphi_{n-1}^+ \varphi_{n-1}^- \varphi_n^+$, $s_n^y = \frac{1}{2\mathrm{i}} \varphi_1^+ \varphi_1^- \ldots \varphi_{n-1}^+ \varphi_{n-1}^- \varphi_n^-$, $s_n^z = -\frac{1}{2} \varphi_n^+ \varphi_n^-$, which are linear combinations of the operators $\eta_k^+$, $\eta_k$, i.e. $\varphi_j^+ = \sum_{k=1}^{N} g_{kj} (\eta_k^+ + \eta_k)$, $\varphi_j^- = \sum_{k=1}^{N} g_{kj} (\eta_k^+ - \eta_k)$. Therefore, the calculation of spin correlation functions reduces to exploiting the Wick–Bloch–de Dominicis theorem. The required elementary contractions have the form

$$\begin{aligned} \langle \varphi_j^+(t) \varphi_m^+ \rangle &= -\langle \varphi_j^-(t) \varphi_m^- \rangle = \sum_{p=1}^{N} g_{pj} g_{pm} \frac{\cosh(\mathrm{i}\Lambda_p t - \frac{\beta \Lambda_p}{2})}{\cosh \frac{\beta \Lambda_p}{2}} \\ \langle \varphi_j^+(t) \varphi_m^- \rangle &= -\langle \varphi_j^-(t) \varphi_m^+ \rangle = \sum_{p=1}^{N} g_{pj} g_{pm} \frac{\sinh(-\mathrm{i}\Lambda_p t + \frac{\beta \Lambda_p}{2})}{\cosh \frac{\beta \Lambda_p}{2}}. \end{aligned} \tag{3}$$

For example, the $xx$ time-dependent spin correlation function can be finally expressed as the Pfaffian of a $2(2j+n-1)\times 2(2j+n-1)$ antisymmetric matrix

$$4\langle s_j^x(t)s_{j+n}^x\rangle = \langle\varphi_1^+(t)\varphi_1^-(t)\ldots\varphi_{j-1}^+(t)\varphi_{j-1}^-(t)\varphi_j^+(t)\varphi_1^+\varphi_1^-\ldots\varphi_{j+n-1}^+\varphi_{j+n-1}^-\varphi_{j+n}^+\rangle$$
$$= \mathrm{Pf}\begin{pmatrix} 0 & \langle\varphi_1^+\varphi_1^-\rangle & \langle\varphi_1^+\varphi_2^+\rangle & \ldots & \langle\varphi_1^+(t)\varphi_{j+n}^+\rangle \\ -\langle\varphi_1^+\varphi_1^-\rangle & 0 & \langle\varphi_1^-\varphi_2^+\rangle & \ldots & \langle\varphi_1^-(t)\varphi_{j+n}^+\rangle \\ \vdots & \vdots & \vdots & \ldots & \vdots \\ -\langle\varphi_1^+(t)\varphi_{j+n}^+\rangle & -\langle\varphi_1^-(t)\varphi_{j+n}^+\rangle & -\langle\varphi_2^+(t)\varphi_{j+n}^+\rangle & \ldots & 0 \end{pmatrix}. \tag{4}$$

Similarly

$$4\mathrm{i}\langle s_j^x(t)s_{j+n}^y\rangle = \langle\varphi_1^+(t)\varphi_1^-(t)\ldots\varphi_{j-1}^+(t)\varphi_{j-1}^-(t)\varphi_j^+(t)\varphi_1^+\varphi_1^-\ldots\varphi_{j+n-1}^+\varphi_{j+n-1}^-\varphi_{j+n}^-\rangle$$
$$= \mathrm{Pf}\begin{pmatrix} 0 & \langle\varphi_1^+\varphi_1^-\rangle & \langle\varphi_1^+\varphi_2^+\rangle & \ldots & \langle\varphi_1^+(t)\varphi_{j+n}^-\rangle \\ -\langle\varphi_1^+\varphi_1^-\rangle & 0 & \langle\varphi_1^-\varphi_2^+\rangle & \ldots & \langle\varphi_1^-(t)\varphi_{j+n}^-\rangle \\ \vdots & \vdots & \vdots & \ldots & \vdots \\ -\langle\varphi_1^+(t)\varphi_{j+n}^-\rangle & -\langle\varphi_1^-(t)\varphi_{j+n}^-\rangle & -\langle\varphi_2^+(t)\varphi_{j+n}^-\rangle & \ldots & 0 \end{pmatrix}. \tag{5}$$

Usually, to discuss the dynamic properties of a spin system one calculates the dynamic structure factor

$$S_{\alpha\beta}(\kappa,\omega) = \sum_{n=1}^{N}\mathrm{e}^{\mathrm{i}\kappa n}\int_{-\infty}^{\infty}\mathrm{d}t\,\mathrm{e}^{-\epsilon|t|}\mathrm{e}^{\mathrm{i}\omega t}\langle s_j^\alpha(t)s_{j+n}^\beta\rangle \qquad \epsilon\to+0 \tag{6}$$

which is related to the corresponding time-dependent spin correlation functions. Another widely used quantity, the dynamic susceptibility $\chi_{\alpha\beta}(\kappa,\omega)$, can be obtained from the dynamic structure factor (6). (Im $\chi_{\alpha\beta}(\kappa,\omega)$ comes from $S_{\alpha\beta}(\kappa,\omega)$ by the fluctuation–dissipation theorem, whereas Re $\chi_{\alpha\beta}(\kappa,\omega)$ comes from Im $\chi_{\alpha\beta}(\kappa,\omega)$ by the Kramers–Kronig transformation (see [28]).) The dynamic properties connected with the $zz$ time-dependent correlation functions are well known [11, 29–33]. Since a $\frac{\pi}{2}$ rotation of all spins about the $z$-axis commutes with Hamiltonian (1) one finds the identities $\langle s_j^y(t)s_{j+n}^y\rangle = \langle s_j^x(t)s_{j+n}^x\rangle$, $\langle s_j^y(t)s_{j+n}^x\rangle = -\langle s_j^x(t)s_{j+n}^y\rangle$. The other correlation functions not mentioned above vanish, and hence it remains to examine the $xx$ and $xy$ time-dependent correlation functions. Alternatively we may examine the correlation functions $\langle s_j^+(t)s_{j+n}^-\rangle$ and $\langle s_j^-(t)s_{j+n}^+\rangle$ since $\langle s_j^x(t)s_{j+n}^x\rangle = \frac{1}{4}(\langle s_j^+(t)s_{j+n}^-\rangle + \langle s_j^-(t)s_{j+n}^+\rangle)$ and $\langle s_j^x(t)s_{j+n}^y\rangle = \frac{\mathrm{i}}{4}(\langle s_j^+(t)s_{j+n}^-\rangle - \langle s_j^-(t)s_{j+n}^+\rangle)$. Due to the translation and reflection invariances that hold for infinite system equation (6) yields

$$\begin{aligned} S_{xx}(\kappa,\omega) &= \sum_{n=0,\pm1,\ldots}\mathrm{e}^{\mathrm{i}\kappa n}2\mathrm{Re}\left[\int_0^\infty\mathrm{d}t\,\mathrm{e}^{\mathrm{i}(\omega+\mathrm{i}\epsilon)t}\langle s_j^x(t)s_{j+n}^x\rangle\right] \\ S_{xy}(\kappa,\omega) &= \sum_{n=0,\pm1,\ldots}\mathrm{e}^{\mathrm{i}\kappa n}2\mathrm{iIm}\left[\int_0^\infty\mathrm{d}t\,\mathrm{e}^{\mathrm{i}(\omega+\mathrm{i}\epsilon)t}\langle s_j^x(t)s_{j+n}^y\rangle\right]. \end{aligned} \tag{7}$$

This form of the quantities of interest is most suitable for further numerical calculation. Further details on the numerical approach can be found in [27].

In our numerical calculations we considered chains of $N=400$ spins with $J=-1$ and the values of transverse field $\Omega = 0,\ldots,2$ at the inverse temperatures $\beta = 100, 20, 5, \ldots, 0$. We calculated $\langle s_j^x(t)s_{j+n}^x\rangle$ and $\langle s_j^x(t)s_{j+n}^y\rangle$ with $j = 41, 51, 61$ and $n$ up to 50 (and up to 100 at $\beta = 20$) evaluating the corresponding Pfaffians (4), (5) constructed from elementary

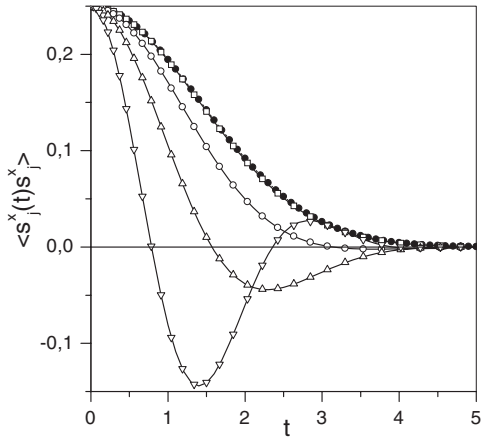


**Figure 1.** Time-dependence of the autocorrelation function $\langle s_j^x(t)s_j^x\rangle$ obtained numerically ($j = 51$) at infinite temperature ($\beta = 0$) for different values of transverse field $\Omega = 2, 1$ (downward and upward triangles), $\Omega = 0.5$ (open circles), $\Omega = 0.1$ (squares), and $\Omega = 0$ (filled circles). Curves represent the exact result (8).

contractions (3), (2) for the times up to $t_c = 250$. Finally, we summed over $n$ and did the integral over $t$ with $\epsilon = 0.001$ (except the case $\Omega = 2$, $\beta = 5$ for which $\epsilon = 0.1$). To estimate the accuracy of the results obtained many additional calculations similar to those described in detail in [27] were performed. They permitted us to assess the finite $N$ and $j$ effects, the effects of termination of the sum over $n$ and of the finite values of $t_c$ and $\epsilon$. The results presented below for $S_{xx}(\kappa, \omega)$ and $S_{xy}(\kappa, \omega)$ pertain to the thermodynamic limit.

Figure 1 shows the time dependence of the autocorrelation function at infinite temperature for some values of the transverse field obtained numerically (symbols) in comparison with the exact analytical result [13, 14] (curves),

$$4\langle s_j^x(t)s_{j+n}^x\rangle = \delta_{n,0}\cos(\Omega t)\mathrm{e}^{-\frac{1}{4}J^2t^2} \qquad (\beta = 0). \tag{8}$$

The figure clearly demonstrates excellent agreement between the analytical and numerical results.

Figure 2 shows numerical results for Re $\langle s_j^x(t)s_j^x\rangle$ at finite temperatures for $\Omega = 0$, along with the asymptotic result [20] valid for long times:

$$\langle s_j^+(t)s_{j+n}^-\rangle \sim \begin{cases} \mathrm{e}^{f(n,0)} & \frac{n}{Jt} > 1 \\ t^{2(\nu_-^2+\nu_+^2)}\mathrm{e}^{f(n,t)} & \frac{n}{Jt} < 1 \end{cases} \tag{9}$$

where

$$f(n,t) = \frac{1}{2\pi}\int_{-\pi}^{\pi} \mathrm{d}p|n + Jt\sin p|\ln\left|\tanh\frac{\beta(\Omega - J\cos p)}{2}\right|$$
$$\nu_\pm = \frac{1}{2\pi}\ln\left|\tanh\frac{\beta\left[\Omega \mp J\sqrt{1-(\frac{n}{Jt})^2}\right]}{2}\right|. \tag{10}$$

From figure 2 one can see that the numerical calculations are in agreement with the analytical predictions (9), (10): for finite temperatures $\langle s_j^x(t)s_j^x\rangle$ decays exponentially (the logarithms of the asymptotics have the same slopes as the logarithms of the computed correlation functions); with increasing temperature one observes Gaussian decay over a time interval of increasing length (see the data for $\beta = 0.000\,01$).

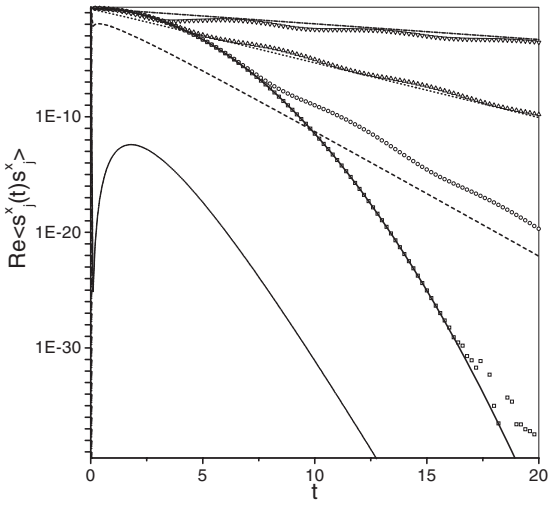


**Figure 2.** Time dependence of the autocorrelation function $\langle s_j^x(t)s_j^x\rangle$ obtained numerically ($j = 51$) for $\Omega = 0$ and various temperatures, on a logarithmic scale. Downward and upward triangles, circles, and squares correspond to the numerical results for $\beta = 5, 1, 0.1$, and 0.000 01, respectively. The exact analytical result for $\beta = 0$ (8) is depicted by a solid curve. Dot-dashed, short-dashed, long-dashed, and dotted curves correspond to the asymptotic result (9), (10) for $\beta = 5, 1, 0.1$, and 0.000 01, respectively. Evidently only the slopes of those asymptotics should be compared with the numerical results. For $\beta = 0.000\,01$ the correlation function does not reach its asymptotic regime within the time range displayed in the figure.

In figure 3 we plotted the numerical result for the low-temperature Fourier transform ($\beta = 100$) of the $xx$ autocorrelation function $\Phi_0^{xx}(\omega) = \int_{-\infty}^{\infty} \mathrm{d}t\, \mathrm{e}^{-\epsilon|t|}\mathrm{e}^{\mathrm{i}\omega t}\langle s_j^x(t)s_j^x\rangle$, $\epsilon \to +0$ which was obtained at $\Omega = 0$ and $\beta = \infty$ in [18] (figure 4 of that paper). To investigate the possible influence of finite-size and boundary effects we studied the time dependence of $\langle s_j^x(t)s_j^x\rangle$ at $\Omega = 0$, $\beta = 100$ up to $t = 300$, (i) for $j = \frac{N}{2} + 1$ in chains of varying length $N$, and (ii) for different $j$ in a $N = 400$ chain. We generally observed a rapid, almost step-like decrease in $\langle s_j^x(t)s_j^x\rangle$ at $t \simeq 2j$, which is often preceded by an increase echoing the initial behaviour of $\langle s_j^x(t)s_j^x\rangle$. As both of these features shift with $j$ they are clearly identifiable as finite-size effects. The wiggles in the low-frequency region of $\Phi_0^{xx}(\omega)$ (figure 3) originate from the step at $t \simeq 200$ in $\langle s_{101}^x(t)s_{101}^x\rangle$ of the $N = 400$ chain. Of course these wiggles may be suppressed by increasing the damping factor $\epsilon$ in the Fourier transform, but that would also blur the sharp spectral features at $\omega = 0$, 1, and 2.

Typical time dependences of spin correlations $\langle s_j^x(t)s_{j+n}^x\rangle$ at finite distance are shown in figure 4. This figure also illustrates the finite-size effects mentioned above, and their temperature dependence. Shown are data for $\mathrm{Re}\,\langle s_j^x(t)s_{j+n}^x\rangle$ for $n = 50$, $j = 41$, 42, and 51 at $\Omega = 0$ and $\beta = 20$ (figure 4($a$)) and $\beta = 100$ (figure 4($b$)). For $\beta = 20$ all data coincide within the line thickness, so that translational invariance is fulfilled within the precision of the figure. However, at $\beta = 100$ translational invariance is definitely broken; the time at which the 'step' occurs shifts by $\Delta t \simeq 20$ as $j$ increases by 10. This demonstrates that finite-size effects become more dangerous at lower temperatures. Figure 4 also demonstrates the generic behaviour of $\langle s_j^x(t)s_{j+n}^x\rangle$ described by the asymptotic formulae (9), (10) which we have verified by comparison with numerical data for various values of the applied field $\Omega$: $\langle s_j^x(t)s_{j+n}^x\rangle$ is a (temperature-dependent) constant up to times $t \simeq n$ and then decays exponentially with superimposed oscillations.

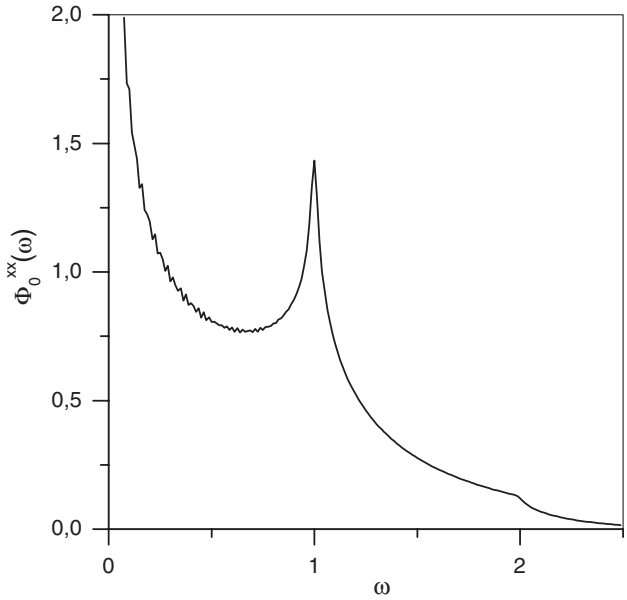


**Figure 3.** Fourier transform of the autocorrelation function $\Phi_0^{xx}(\omega)$ in the absence of the transverse field at low temperature $\beta = 100$ computed with $j = 101$, $t_c = 300$, $\epsilon = 0.001$.

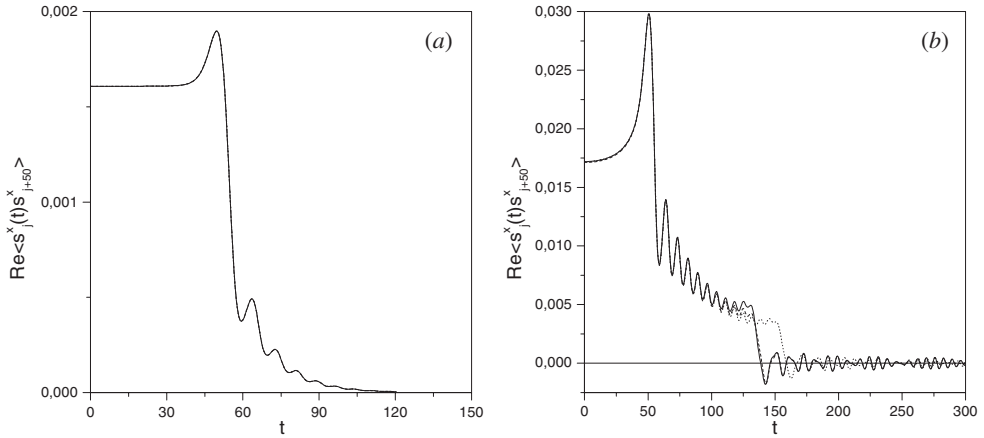


**Figure 4.** Dependence of $\mathrm{Re}\langle s_j^x(t)s_{j+50}^x\rangle$ ($N = 400$) on time at the low temperatures $\beta = 20$ (*a*) and $\beta = 100$ (*b*) for $\Omega = 0$ with $j = 41$ (solid curves), $j = 42$ (dashed curves), $j = 51$ (dotted curves).

## 3. The dynamic structure factor

This section contains our main results. The data for the dynamic structure factors $S_{xx}(\kappa, \omega)$ and $S_{xy}(\kappa, \omega)$ which we present in figures 5–10 are the first finite-temperature and finite-field results available for these quantities, apart from zero-field results from a complete diagonalization of short ($N \leqslant 16$) closed chains [34]. For comparison of the new results for the $xx$ and $xy$ dynamics with the known results concerning the $zz$ dynamics we present in figure 11 the low-temperature dependence of the $zz$ dynamic structure factor on the wavevector and frequency for several values of the transverse field.

It should be noted that our results apply to ferromagnetic ($J < 0$) as well as antiferromagnetic ($J > 0$) coupling, since $\langle s_j^x(t)s_{j+n}^x\rangle$ and $\langle s_j^x(t)s_{j+n}^y\rangle$ for $J > 0$ differ from the same correlation functions for $J < 0$ only by the factor $(-1)^n = \mathrm{e}^{\pm \mathrm{i}\pi n}$. Therefore, it follows from equation (6) that $S_{xx}(\pi - \kappa, \omega)$ and $S_{xy}(\pi - \kappa, \omega)$ for the antiferromagnet are equal to $S_{xx}(\kappa, \omega)$ and $S_{xy}(\kappa, \omega)$ for the ferromagnet, respectively, and hence it is sufficient to study only one case, e.g. that of ferromagnetic coupling.

Let us now discuss the numerical results, starting with the dynamic structure factor $S_{xx}(\kappa, \omega)$ at low temperature, $\beta = 20$ (figure 5). At small values of the wavevector (e.g. $\kappa = \frac{\pi}{8}$) the frequency dependence of $S_{xx}(\kappa, \omega)$ has a one-peak structure for all values of $\Omega$. For larger values of $\kappa$ the frequency dependence of $S_{xx}(\kappa, \omega)$ becomes more complicated essentially depending on the value of the transverse field. With increasing $\Omega$ one-peak (for $\kappa = \frac{\pi}{4}$) or two-peak (for $\kappa = \frac{\pi}{2}$, $\kappa = \frac{2\pi}{3}$, $\kappa = \frac{3\pi}{4}$, $\kappa = \pi$) frequency profiles transform into two-peak or three-peak (e.g. for $\kappa = \frac{2\pi}{3}$) profiles and finally back into one-peak profiles. From figure 5 one can see that with increasing $\kappa$ the frequency profile of $S_{xx}(\kappa, \omega)$ transforms from one-peak type to two-peak type at $\Omega = 0.001$, 0.9 or from one-peak type through two-peak type to three-peak type and then to two-peak type at $\Omega = 0.1,\ 0.5, 0.75$. At $\Omega = 1$ (or larger) the frequency profiles of $S_{xx}(\kappa, \omega)$ have one-peak structure for all $\kappa$.

$\Omega = 1$ is the critical field strength above which the ground state of the chain is ferromagnetically saturated; consequently there are no qualitative changes in the excitation spectrum and in the dynamic structure factors for $\Omega > 1$. In contrast, the ground state changes with $\Omega$ for $\Omega < 1$. This is evident in the changes in the low-lying excitations visible in figure 5, to be discussed shortly.

Figures 6–9 illustrate the temperature dependence of $S_{xx}(\kappa, \omega)$. At $\Omega = 0.1$, 0.5 and $\beta = 5$ one can still observe a transformation in the $\omega$-dependence of $S_{xx}(\kappa, \omega)$ from one-peak profiles to 'two-peak' profiles as $\kappa$ increases; at $\beta = 1$ one finds only one peak that spreads and slightly moves towards higher frequencies with increasing $\kappa$; at $\beta = 0.1$ there is only one broad $\kappa$-independent maximum in the frequency dependence of $S_{xx}(\kappa, \omega)$. For larger values of the transverse field $\Omega = 1$, 2, $S_{xx}(\kappa, \omega)$ always exhibits a one-peak frequency profile that moves towards higher frequencies with increasing $\kappa$ at $\beta = 5$, 1, and does not depend on $\kappa$ at the high temperature $\beta = 0.1$. The single broad $\kappa$-independent Gaussian ridge at $\beta = 0.1$ in any of figures 6–9 represents the Fourier transform of equation (8). Note that the $\kappa$-independence of $S_{xx}(\kappa, \omega)$ is a very general feature, as $\langle s_j^x(t)s_{j+n}^x\rangle$, $n \neq 0$ vanishes in the high-temperature limit for completely arbitrary (e.g. inhomogeneous or random) spin-$\frac{1}{2}$ $XY$ chains. However, for some of the few known cases (besides the one treated here) in which $\beta = 0$ correlations may be calculated explicitly (see [15] for several results and a review of previous work) up to three Gaussian peaks (modulated by periodic functions) may show up.

Figure 10 shows $\mathrm{i}S_{xy}(\kappa, \omega)$ at low temperature ($\beta = 20$) for various values of $\Omega$. For $\Omega = 0$, $\mathrm{i}S_{xy}(\kappa, \omega)$ vanishes due to spin-flip symmetry. In contrast to $S_{xx}(\kappa, \omega)$, $\mathrm{i}S_{xy}(\kappa, \omega)$ need not be positive, and for small $\Omega$ values it displays an interesting pattern of ridges and valleys. For large $\Omega$ values $\mathrm{i}S_{xy}(\kappa, \omega)$ resembles $S_{xx}(\kappa, \omega)$ more and more closely.

It is useful to compare the new low-temperature results for $S_{xx}(\kappa, \omega)$ and $S_{xy}(\kappa, \omega)$ (figures 5, 10) with those long known for $S_{zz}(\kappa, \omega)$ (figure 11). $S_{zz}(\kappa, \omega)$ originates from two excitation continua [31, 35, 36] whose boundaries are visible in figure 11. The continua represent two-particle excitations of the Jordan–Wigner fermions. As the single-fermion dispersion relation is bounded the continua have sharp upper frequency cutoffs at which $S_{zz}(\kappa, \omega)$ may diverge. At $\beta = \infty$ there is also a sharp lower frequency cutoff which touches the line $\omega = 0$ at $\kappa = 0$ and a second field-dependent 'soft-mode' wavenumber, $\kappa_c = 2 \arccos \Omega$. With increasing temperature the lower frequency cutoff becomes smeared

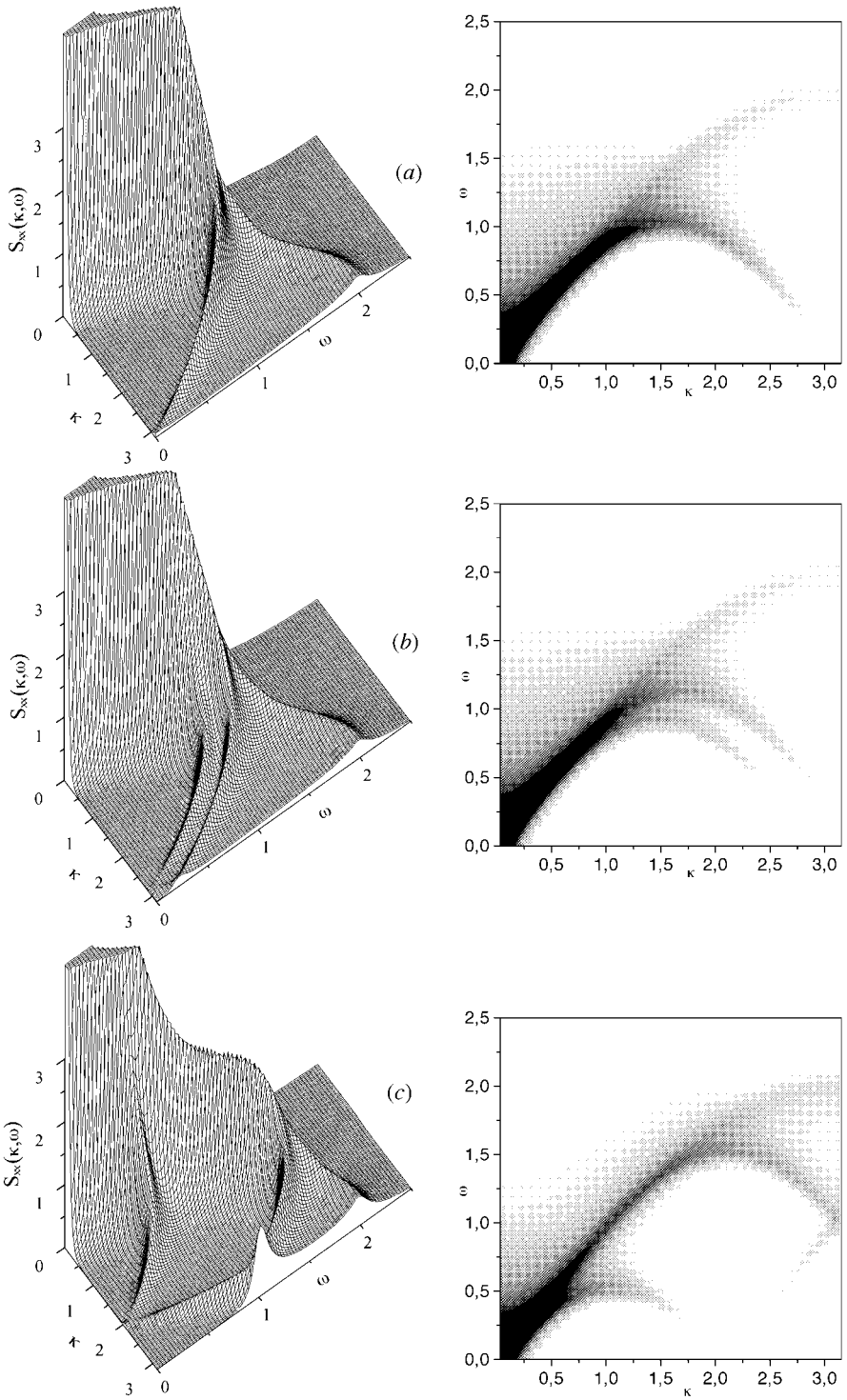


**Figure 5.** $S_{xx}(\kappa, \omega)$ for $\Omega = 0.001$ (*a*), $\Omega = 0.1$ (*b*), $\Omega = 0.5$ (*c*), $\Omega = 0.75$ (*d*), $\Omega = 0.9$ (*e*), $\Omega = 1$ (*f*) at the temperature $\beta = 20$.

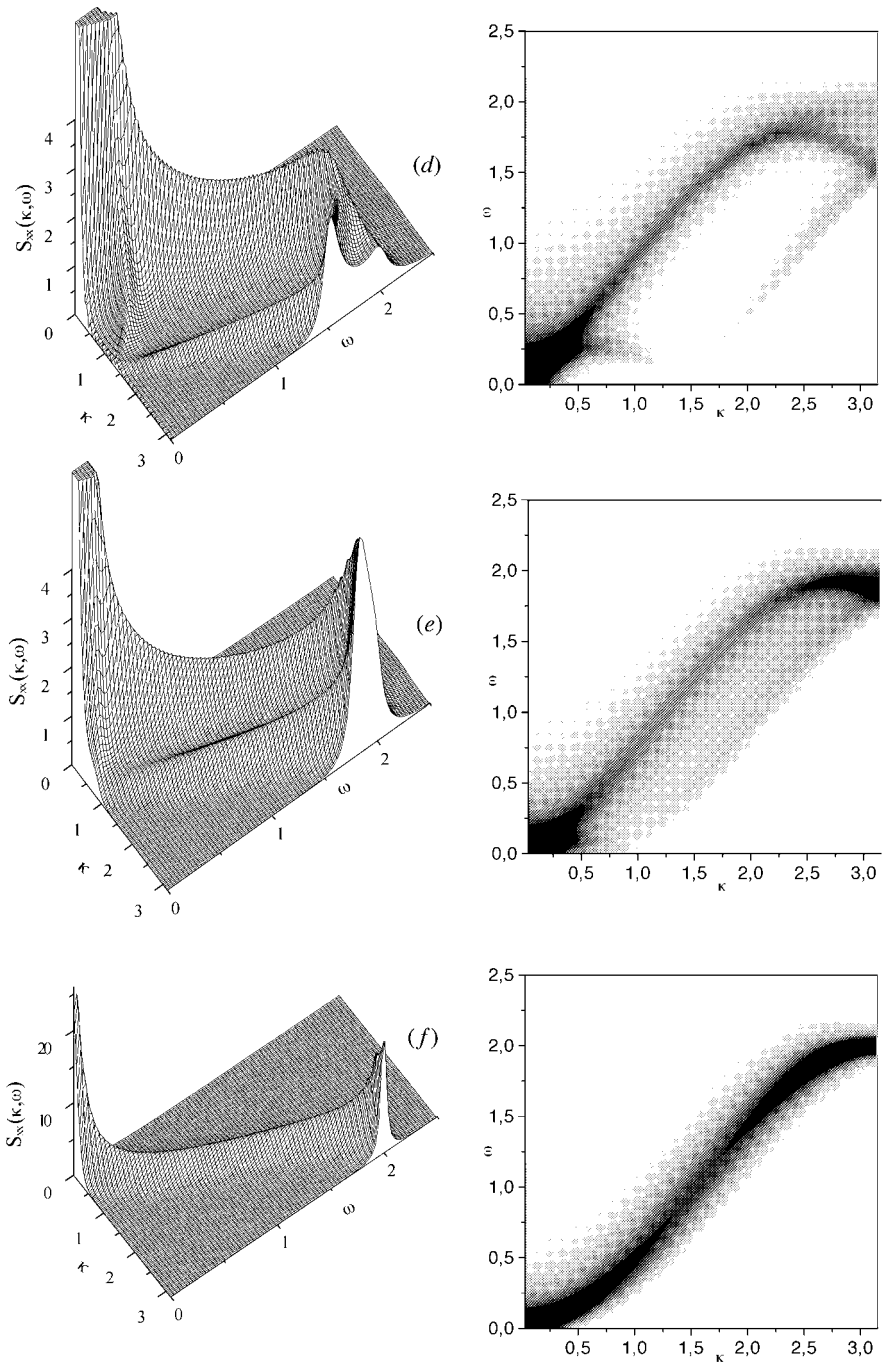


**Figure 5.** (Continued)

out and finally disappears. The transverse field Ω corresponds to the chemical potential of the Jordan–Wigner fermions which becomes irrelevant at infinite temperature. Thus $S_{zz}(\kappa, \omega)$ becomes Ω-independent at $\beta = 0$, but still depends on $\kappa$. In contrast (as discussed above)

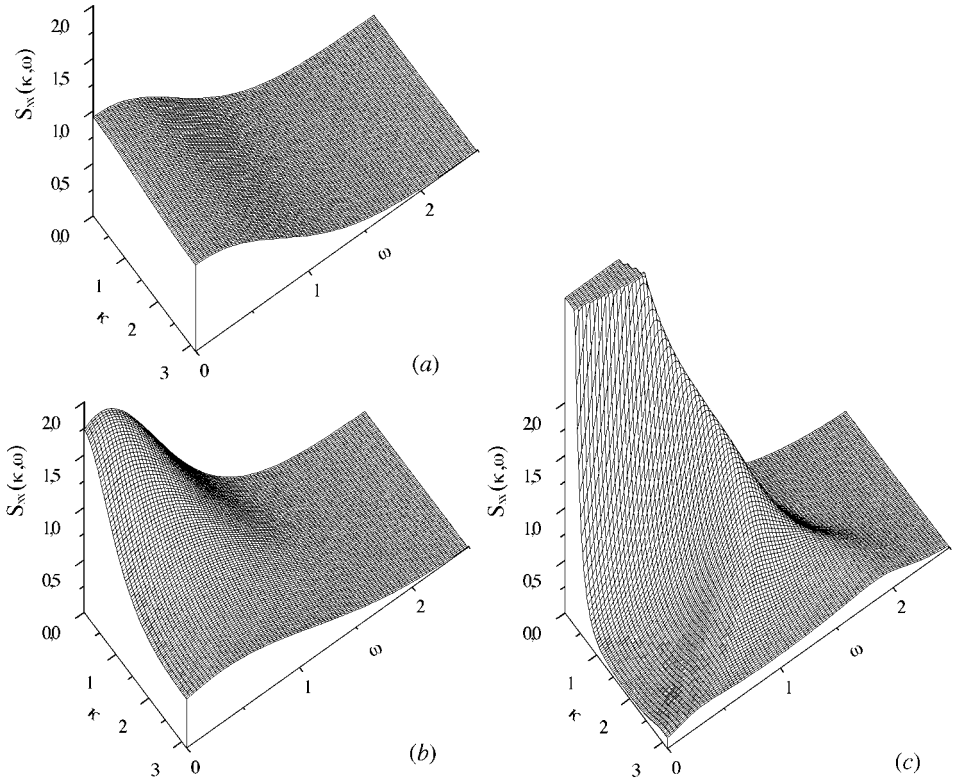


**Figure 6.** Temperature dependence of $S_{xx}(\kappa, \omega)$ for $\Omega = 0.1$: $\beta = 0.1$ $(a)$, $\beta = 1$ $(b)$, $\beta = 5$ $(c)$.

$S_{xx}(\kappa, \omega)$ becomes $\kappa$-independent at $\beta = 0$ but still depends on $\Omega$. In comparison to $S_{zz}(\kappa, \omega)$, much less is known about the structure factors $S_{xx}(\kappa, \omega)$ and $\mathrm{i}S_{xy}(\kappa, \omega)$, which are many-particle quantities in terms of the Jordan–Wigner fermions, as is obvious from the discussion in section 2. Therefore the frequency range of $S_{xx}(\kappa, \omega)$ and $\mathrm{i}S_{xy}(\kappa, \omega)$ is not *a priori* restricted and spectral weight might be expected throughout the $(\kappa, \omega)$ plane. However, as already observed for the spin-$\frac{1}{2}$ $XXZ$ chain [34], $S_{xx}(\kappa, \omega)$ does not meet these expectations; it is rather small (but not zero) outside the excitation continua shown in figure 11, and it shows washed-out excitation branches roughly following the boundaries of the excitation continua. In contrast, $S_{zz}(\kappa, \omega)$ is (apart from boundary singularities) almost structureless inside the excitation continua and strictly zero outside. These findings are illustrated, for example, by figures 5$(c)$, 10$(c)$, and 11$(c)$ (for $\Omega = 0.5$). Comparing, for example, figures 5$(a)$, $(b)$ and 11$(a)$, $(b)$ one finds that a nonzero transverse field $\Omega$ generates an additional excitation branch in $S_{xx}(\kappa, \omega)$ which closely follows the lower frequency cutoff for $S_{zz}(\kappa, \omega)$ whose soft-mode behaviour was discussed in [35]. Figures 10 and 5 show that in general $\mathrm{i}S_{xy}(\kappa, \omega)$ and $S_{xx}(\kappa, \omega)$ have many spectral features in common, however, the physical meaning of the former quantity is less obvious.

It is interesting to compare our numerical results with the analytical predictions of the bosonization method which exploits the bosonic nature of low-lying excitations in a weakly interacting one-dimensional Fermi system. The fermionic dispersion relation can be linearized about the Fermi momentum and the continuum limit is performed as only long-

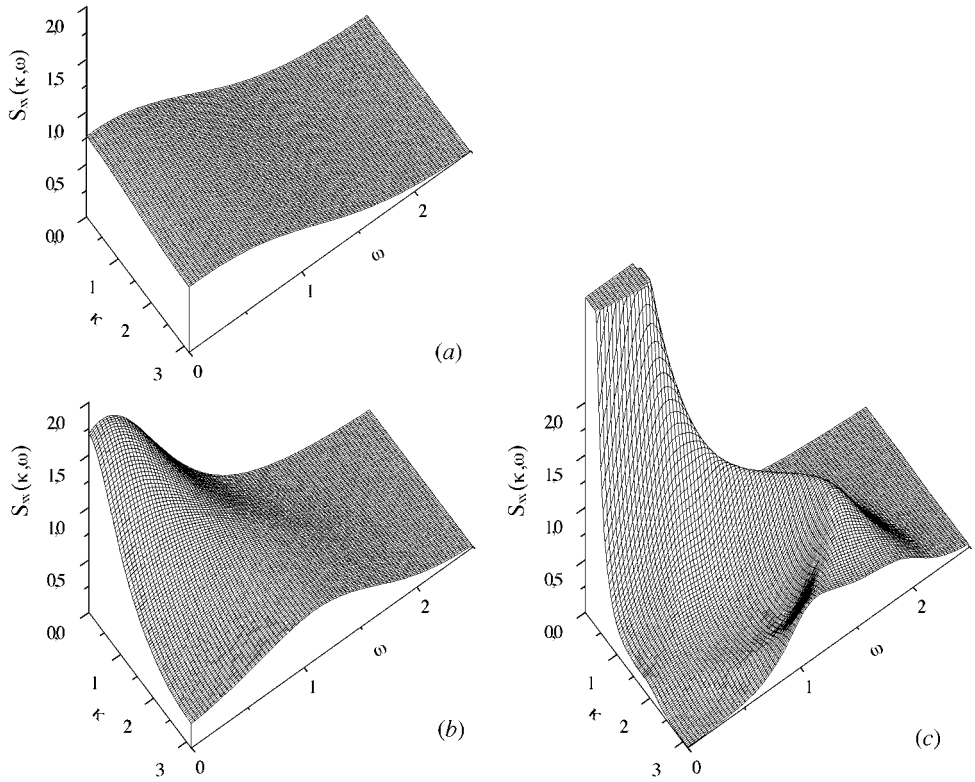


**Figure 7.** The same as in figure 6 for $\Omega = 0.5$.

wavelength excitations are considered. For the spin-$\frac{1}{2}$ $XXZ$ chain (as mapped to interacting fermions by a Jordan–Wigner transformation) the pioneering work was done by Luther and Peschel [37] for $\beta = \infty$; Schulz [38] generalized their work to finite temperature and higher spin quantum numbers. As a continuum theory focused on low-energy excitations, bosonization fails to describe high-frequency phenomena (e.g. cutoffs) in dynamic structure factors which are related to the boundedness of lattice fermion spectra. This was observed [34], for example, when finite-temperature bosonization results for the dynamic structure factor of a spin-$\frac{1}{2}$ Heisenberg antiferromagnet were compared with numerical data from complete diagonalization of 16-spin chains.

The $\beta = \infty$ structure factors of the isotropic $XY$ chain (with no external field) as obtained by bosonization are

$$S_{\mu\mu}(\kappa,\omega) \sim \frac{\theta(\omega - |v\kappa|)}{[\omega^2 - (v\kappa)^2]^{1-\frac{\eta_\mu}{2}}} \qquad (\mu = x, z) \tag{11}$$

where the spinon velocity $v = J$ equals the Fermi velocity of the Jordan–Wigner fermions. The singularity exponents $\eta_x = \frac{1}{\eta_z} = \frac{1}{2}$ describe correctly the known singularities at the lower continuum boundary. However, due to linearization of the fermion dispersion, the lower continuum boundary $\varepsilon_l(\kappa) = J \sin\kappa$ is only approximated well for $\kappa$ close to 0 or $\pi$ as follows from (11). A magnetic field in the $z$ direction corresponds to a chemical potential for the Jordan–Wigner fermions. This does not cause any qualitative changes in the bosonization calculation; only the values of the Fermi momentum and Fermi velocity are changed. The

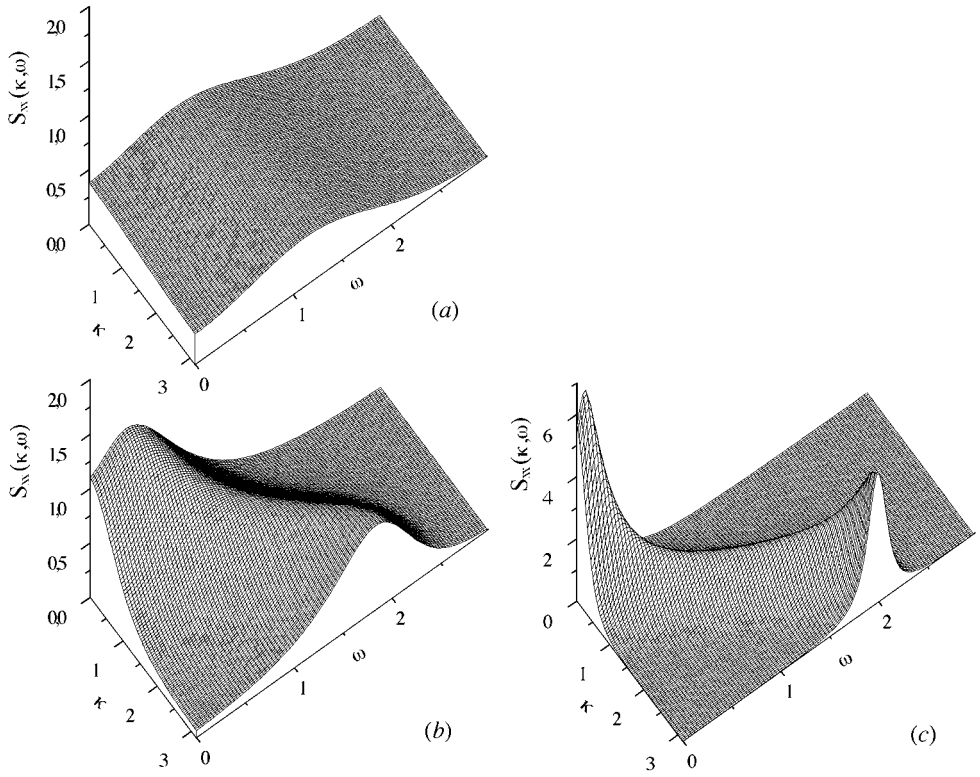


**Figure 8.** The same as in figure 6 for $\Omega = 1$.

resulting changes in the continuum boundaries (for $S_{zz}(\kappa, \omega)$) were discussed by Taylor and Müller [31] and are illustrated in figure 11.

The divergence of $S_{xx}(\kappa, \omega)$ (smoothed by numerical effects) at the lower continuum boundary is clearly visible in our low-temperature data, along with high-frequency singularities not accounted for by bosonization. The magnetic-field induced soft mode at $\kappa_c$ shows up as a sharp V-shaped ridge in $S_{xx}(\kappa, \omega)$. At higher temperature bosonization predicts a softening of the continuum boundary singularities in accordance with our numerical data.

The excitations of the system can be discussed in terms of the retarded temperature double-time Green function [28] $\mathcal{G}^{-}_{j,j+n}(t) = -\mathrm{i}\theta(t)\langle[s^{-}_{j}(t), s^{+}_{j+n}]\rangle$. Its Fourier transform with respect to time $t$ and distance $n$ $\mathcal{G}^{-}_{\kappa}(\omega) = \sum_{n=1}^{N} \mathrm{e}^{\mathrm{i}\kappa n} \int_{-\infty}^{\infty} \mathrm{d}t\, \mathrm{e}^{\mathrm{i}(\omega+\mathrm{i}\epsilon)t}\mathcal{G}^{-}_{j,j+n}(t)$, $\epsilon \to +0$ is equal to the dynamic susceptibility $\chi_{-+}(\kappa, \omega)$. From the fluctuation–dissipation theorem in the limit of low temperatures $S_{-+}(\kappa, \omega) \sim -\mathrm{Im}\,\chi_{-+}(\kappa, \omega)$, $\omega \neq 0$. Assuming $s^{+}_{n}$, $s^{-}_{n}$ to obey Bose commutation rules one immediately finds for the spin model defined by (1) that $\chi_{-+}(\kappa, \omega) = 1/(\omega - \Omega - J\cos\kappa + \mathrm{i}\epsilon)$ or that $S_{-+}(\kappa, \omega) \sim \delta(\omega - \Lambda_{\kappa})$, $\Lambda_{\kappa} = \Omega + J\cos\kappa$, i.e. the dynamic structure factor for given $\kappa$ shows a single peak corresponding to a magnon branch with dispersion $\Lambda_{\kappa}$. This result coincides with the exact one [39] obtained for $\beta = \infty$, $\Omega > J$, but it is qualitatively wrong for $\Omega < J$ as our numerical results demonstrate: they often show multiple peaks, continua, etc. Figures 5 and 10 show that in many situations the dominant contributions to the dynamic structure factor $S_{-+}(\kappa, \omega)$ can be described by a small number of broadened excitation branches. However, the kind of single-mode approximation described above will in most cases be inappropriate for deriving the magnetic excitation spectrum from scattering experiments.

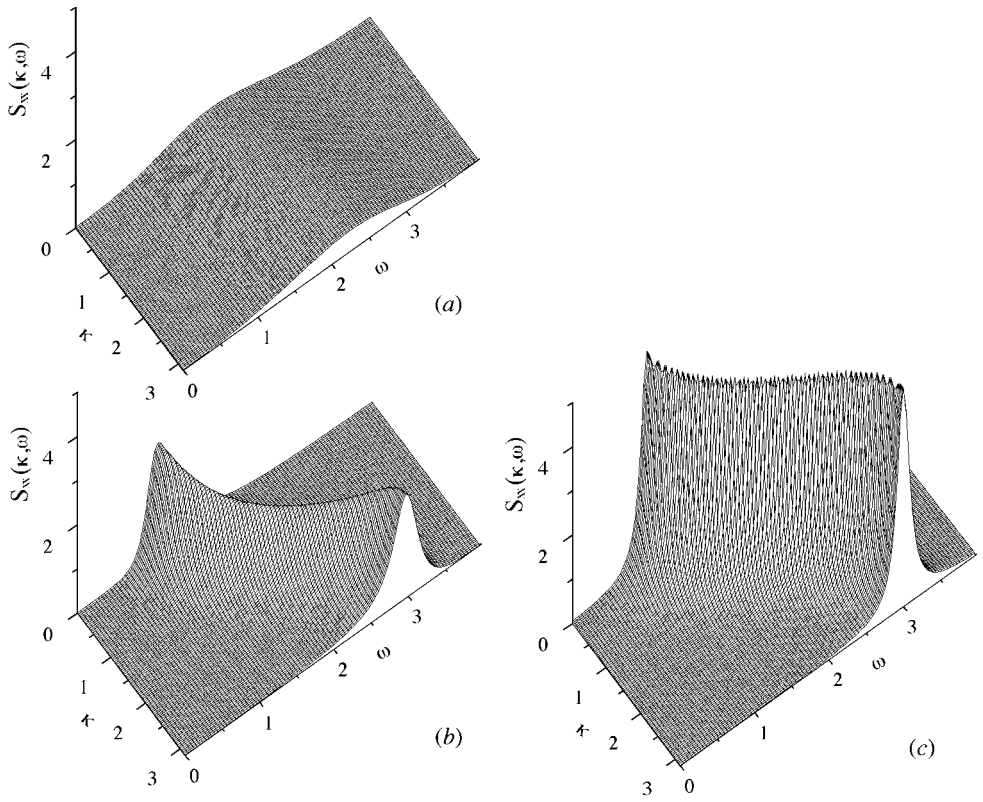


**Figure 9.** The same as in figure 6 for $\Omega = 2$.

## 4. An experimental application

As an application of our results let us discuss the temperature dependence of the spin–spin relaxation time in $PrCl_3$ which was not known heretofore due to lack of information about the $xx$ time-dependent correlation functions for the spin-$\frac{1}{2}$ $XY$ chain [7]. The Pr–Pr interaction in this compound (as derived from measurements of static quantities) can be reasonably described by the model (1) with $J/k_B = 2.85$ K and $\Omega = 0$, and the spin–spin relaxation time $T_2$ is related [7] to the $xx$ time-dependent autocorrelation function

$$\frac{1}{T_2} \sim \int_{-\infty}^{\infty} \mathrm{d}t \, \langle s_j^x(t) s_j^x \rangle. \tag{12}$$

The result of our calculation is shown in figure 12. $T_2$ is an increasing function of temperature and crosses over to a constant at about 1 K. The plateau in the temperature dependence of $T_2$ (12) can be understood from our results presented above. For the time range during which $\langle s_j^x(t) s_j^x \rangle$ contributes appreciably to the integral (12), it does not depend on temperature for sufficiently high temperatures. This can be seen in figure 2: the data for $\beta \leqslant 1$ coincide in the region where $\langle s_j^x(t) s_j^x \rangle$ has non-negligible values; the differences between high and infinite temperatures occur only at long times, where $\langle s_j^x(t) s_j^x \rangle$ is already very small.

Qualitatively, our result for the temperature dependence is similar to that of an earlier short-chain calculation [7] and to the behaviour observed experimentally [7]; however, there are

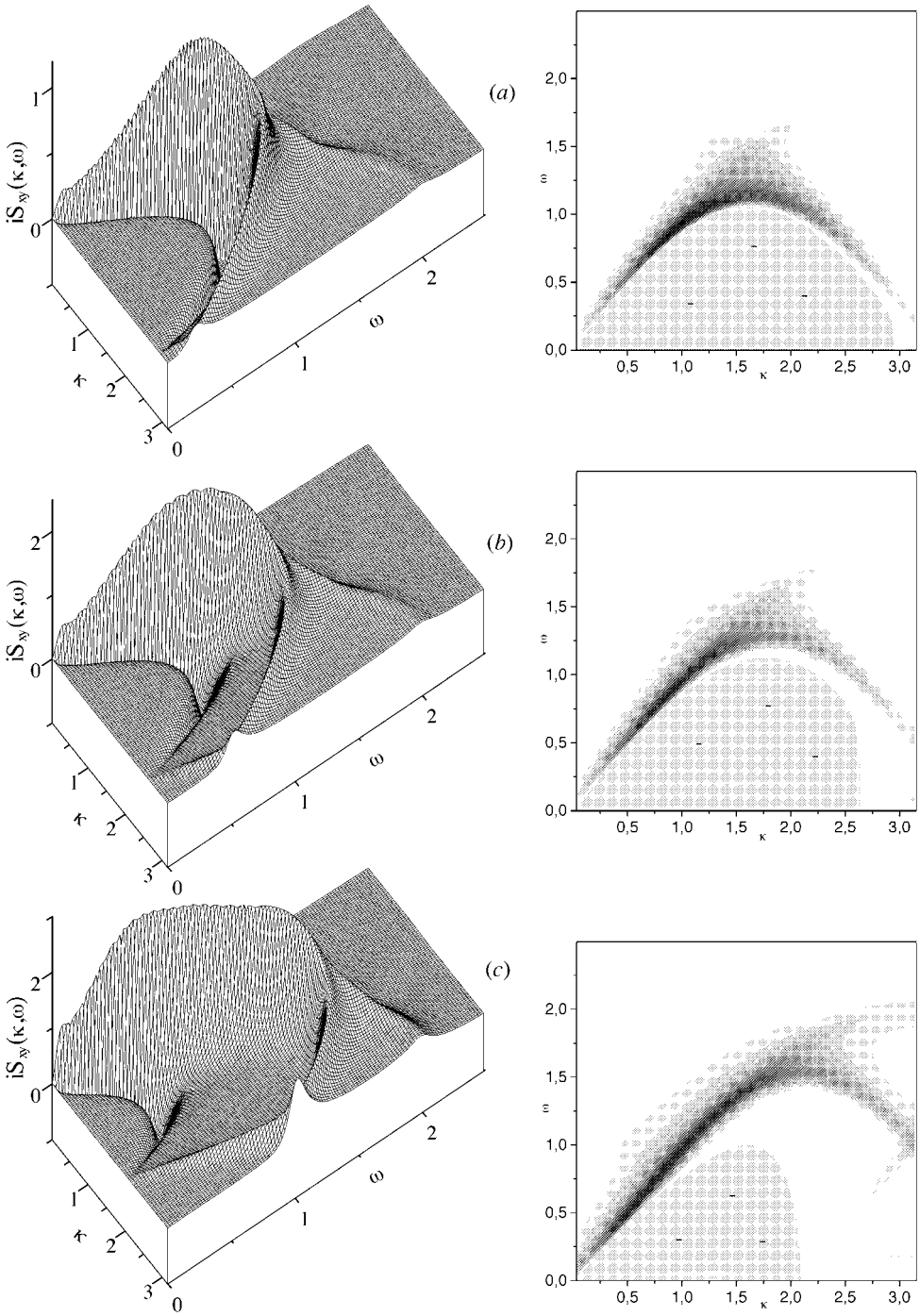


**Figure 10.** $\mathrm{i}S_{xy}(\kappa,\omega)$ for $\Omega=0.1$ (*a*), $\Omega=0.25$ (*b*), $\Omega=0.5$ (*c*), $\Omega=0.75$ (*d*), $\Omega=0.9$ (*e*), $\Omega=1$ (*f*) at $\beta=20$. In the regions denoted by minuses $\mathrm{i}S_{xy}(\kappa,\omega)<0$.

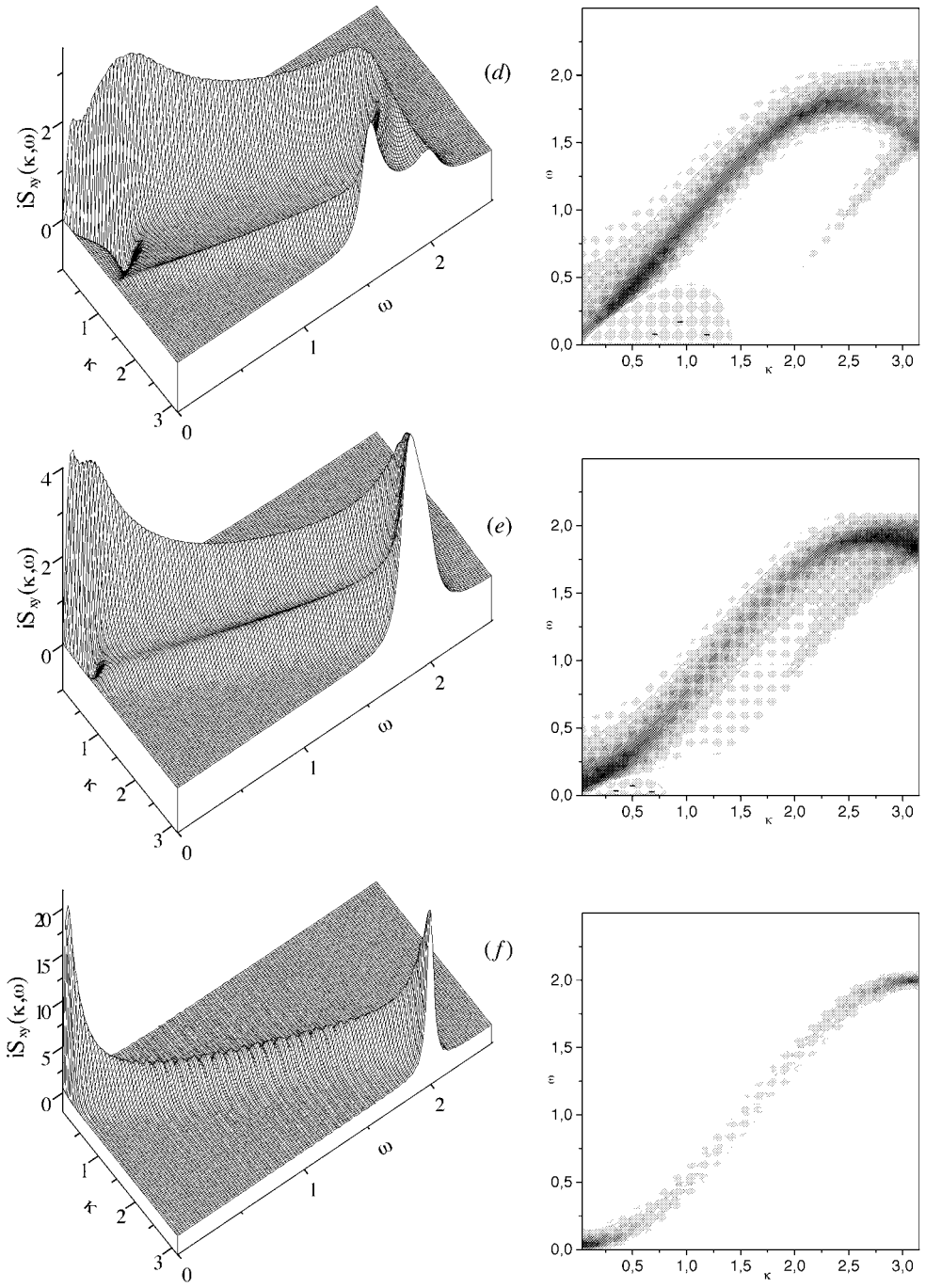


**Figure 10.** (Continued)

significant discrepancies in the value of the crossover temperature. The short-chain calculation yields a crossover at less than 2.5 K; additional approximations (artificial coarse-graining in $\omega$) were necessary in that calculation to extrapolate from $N = 10$, 12 to $N = \infty$. The

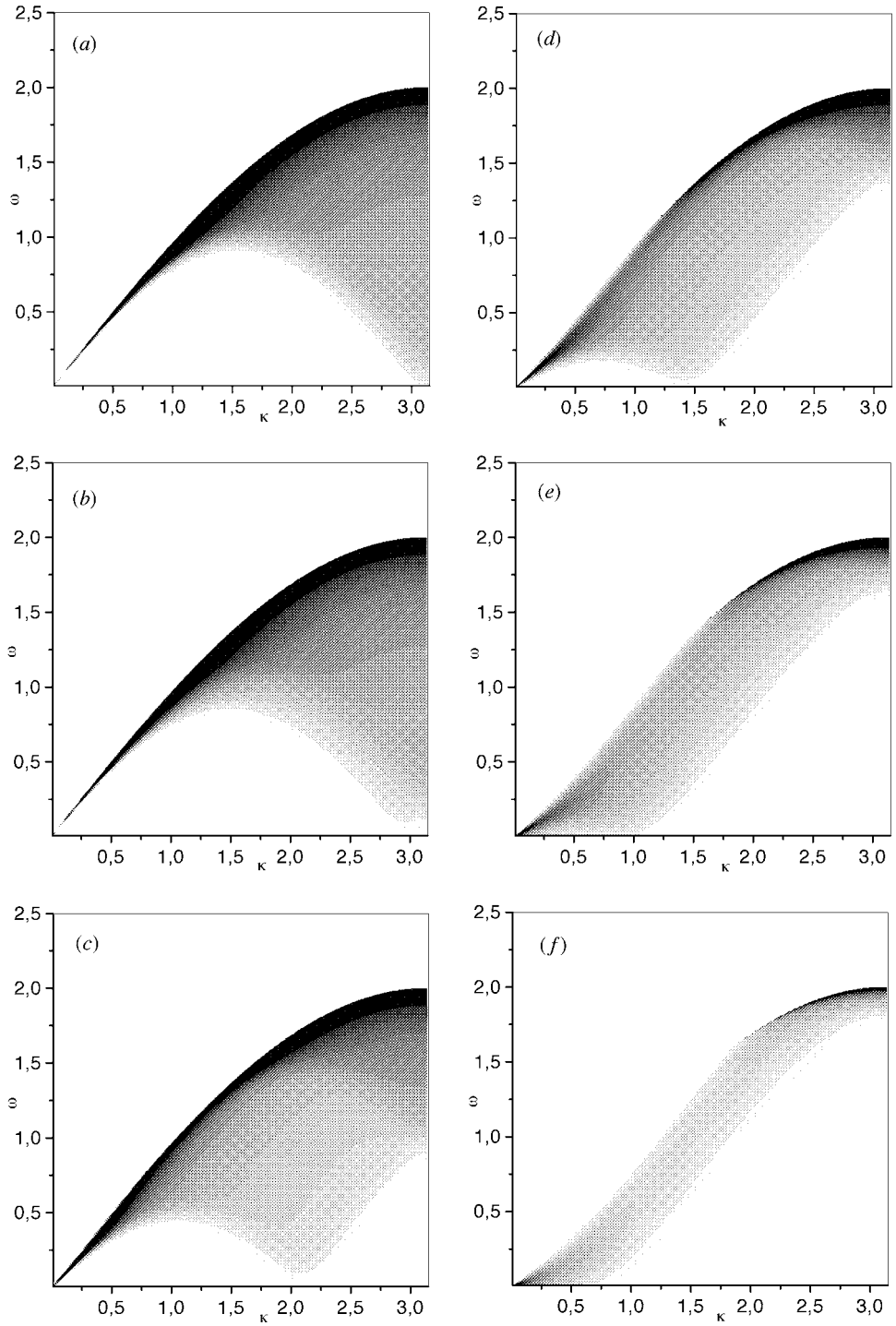


**Figure 11.** Greyscale plots of $S_{zz}(\kappa, \omega)$ for $\Omega = 0.001$ (*a*), $\Omega = 0.1$ (*b*), $\Omega = 0.5$ (*c*), $\Omega = 0.75$ (*d*), $\Omega = 0.9$ (*e*), $\Omega = 1$ (*f*) at $\beta = 20$.

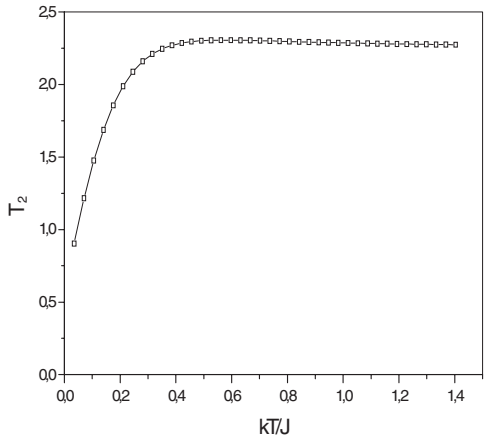


**Figure 12.** Temperature dependence of the spin–spin relaxation time (12): long-chain calculation result. The squares denote the numerical results; the connecting curve is a guide to the eye.

experimental crossover temperature of 6 K is still much higher. This indicates (as already suspected earlier [7]) that while the static thermal behaviour of $PrCl_3$ may be describable by an isotropic $XY$ chain with $J/k_B = 2.85$ K, the dynamics is probably more complicated.

To summarize, we have computed the $xx$ and $xy$ time-dependent spin correlation functions for the spin-$\frac{1}{2}$ isotropic $XY$ chain in a transverse field and the corresponding dynamic structure factors. Our investigations have indicated excitations that govern the dynamic structure factors in the spin-$\frac{1}{2}$ isotropic $XY$ chain in a transverse field. Our results should be useful for understanding dynamic experiments on quasi-one-dimensional spin-$\frac{1}{2}$ $XY$-like compounds. As an obviously interesting extension of the present study, a chain with regularly alternating couplings may be studied. Systems of this kind are discussed in adiabatic treatments of the spin–Peierls transition as well as in modelling structurally dimerized spin chain compounds and have recently been discussed intensively, see [40] and references cited therein. Work in this direction is in progress.

## Acknowledgments

The authors are grateful to Professor G Müller for useful comments, Professor J Richter for discussions, and Professor M Shovgenyuk for providing the possibility to perform part of the numerical calculations. OD acknowledges the kind hospitality of the University of Dortmund in the autumn of 1998 when the present study was initiated.

## References

[1] Lieb E, Schultz T and Mattis D 1961 *Ann. Phys., NY* **16** 407
[2] Plascak J A, Sá Barreto F C and Pires A S T 1983 *Phys. Rev.* B **27** 523
Plascak J A, Pires A S T and Sá Barreto F C 1982 *Solid State Commun.* **44** 787
[3] Watarai S and Matsubara T 1984 *Prog. Theor. Phys.* **71** 840
Watarai S and Matsubara T 1984 *J. Phys. Soc. Japan* **53** 3648
[4] Levitsky R R, Grigas J, Zachek I R, Mits Ye V and Paprotny W 1986 *Ferroelectrics* **67** 109
Levitskii R R, Sokolovskii R O and Sorokov S I 1997 *Condensed Matter Physics (L'viv)* **10** 67
[5] de Carvalho A V and Salinas S R 1978 *J. Phys. Soc. Japan* **44** 238
[6] Zinenko V I 1979 *Fiz. Tverd. Tela* **21** 1819 (Engl. Transl. 1979 *Sov. Phys.–Solid State* **21** 1041)

[7] D'Iorio M, Armstrong R L and Taylor D R 1983 *Phys. Rev.* B **27** 1664
D'Iorio M, Glaus U and Stoll E 1983 *Solid State Commun.* **47** 313
[8] Alistratov A L, Stefanovskii E P and Yablonskii D A 1990 *Fiz. Nizk. Temp.* **16** 1306 (Engl. Transl. 1990 *Sov. J. Low Temp. Phys.* **16** 749)
Voronkova V K, Mosina L V, Usachev A E and Yablokov Yu V 1993 *Fiz. Tverd. Tela* **35** 1114 (Engl. Transl. 1993 *Sov. Phys.–Solid State* **35** 569)
[9] Collins M F and Petrenko O A 1997 *Can. J. Phys.* **75** 605
[10] Knoester J 1993 *J. Chem. Phys.* **99** 8466
Suzuura H, Tokihiro T and Ota Y 1994 *Phys. Rev.* B **49** 4344
[11] Niemeijer Th 1967 *Physica* **36** 377
[12] McCoy B M, Barouch E and Abraham D B 1971 *Phys. Rev.* A **4** 2331
[13] Brandt U and Jacoby K 1976 *Z. Phys.* B **25** 181
Brandt U and Jacoby K 1977 *Z. Phys.* B **26** 245
[14] Capel H W and Perk J H H 1977 *Physica* A **87** 211
[15] Perk J H H and Capel H W 1980 *Physica* A **100** 1
[16] Cruz H B and Gonçalves L L 1981 *J. Phys. C: Solid State Phys.* **14** 2785
[17] McCoy B M, Perk J H H and Shrock R E 1983 *Nucl. Phys.* B **220** 35
McCoy B M, Perk J H H and Shrock R E 1983 *Nucl. Phys.* B **220** 269
[18] Müller G and Shrock R E 1984 *Phys. Rev.* B **29** 288
[19] Colomo F, Izergin A G, Korepin V E and Tognetti V 1992 *Phys. Lett.* A **169** 243
[20] Its A R, Izergin A G, Korepin V E and Slavnov N A 1993 *Phys. Rev. Lett.* **70** 1704
[21] Colomo F, Izergin A G and Tognetti V 1997 *J. Phys. A: Math. Gen.* **30** 361
[22] Ilinski K N and Kalinin G V 1996 *Phys. Rev.* E **54** R1017
[23] Ilinskaia A V, Ilinski K N, Kalinin G V, Melezhik V V and Stepanenko A S 1995 *Preprint* cond-mat/9509040
[24] Farias G A and Gonçalves L L 1987 *Phys. Status Solidi* B **139** 315
[25] Stolze J, Nöppert A and Müller G 1995 *Phys. Rev.* B **52** 4319
[26] Sachdev S and Young A P 1997 *Phys. Rev. Lett.* **78** 2220
[27] Derzhko O and Krokhmalskii T 1997 *Phys. Rev.* B **56** 11659
Derzhko O and Krokhmalskii T 1998 *Phys. Status Solidi* B **208** 221
[28] Zubarev D N 1971 *Njeravnovjesnaja Statistitchjeskaja Tjermodinamika* (Moscow: Nauka) (Engl. Transl. 1974 *Nonequilibrium Statistical Thermodynamics*) (New York: Consultants Bureau)
[29] Katsura S, Horiguchi T and Suzuki M 1970 *Physica* **46** 67
[30] Gersch H A 1970 *Phys. Rev.* B **1** 2270
[31] Taylor J H and Müller G 1985 *Physica* A **130** 1
[32] Viswanath V S and Müller G 1994 *The Recursion Method: Application to Many-Body Dynamics* (Berlin: Springer)
[33] Derzhko O and Krokhmalskii T 2000 *Phys. Status Solidi* B **217** 927
[34] Fabricius K, Löw U and Stolze J 1997 *Phys. Rev.* B **55** 5833
[35] Müller G, Thomas H, Beck H and Bonner J 1981 *Phys. Rev.* B **24** 1429
[36] Müller G, Thomas H, Puga M W and Beck H 1981 *J. Phys. C: Solid State Phys.* **14** 3399
[37] Luther A and Peschel I 1975 *Phys. Rev.* B **12** 3908
[38] Schulz H J 1986 *Phys. Rev.* B **34** 6372
[39] Gonçalves L L 1986 *Rev. Bras. Fis.* **16** 491
[40] Yu W and Haas S 1999 *Preprint* cond-mat/9909093 (*Phys. Rev.* B submitted)